Journal of Earthquake Engineering

ISSN: (Print) (Online) Journal homepage: www.tandfonline.com/journals/ueqe20

Characterization of Site Amplification by a Parametric Study

N. Özge Fercan, Erdal Şafak & Atilla Ansal

To cite this article: N. Özge Fercan, Erdal Şafak & Atilla Ansal (06 Nov 2023): Characterization of Site Amplification by a Parametric Study, Journal of Earthquake Engineering, DOI: 10.1080/13632469.2023.2277833

To link to this article: https://doi.org/10.1080/13632469.2023.2277833

Published online: 06 Nov 2023.

JOURNAL OF EARTHQUAKE ENGINEERING
https://doi.org/10.1080/13632469.2023.2277833

Characterization of Site Amplification by a Parametric Study

N. Özge Fercan [a], Erdal Şafak [b], and Atilla Ansal [c]

[a]Civil Engineering Department, Istanbul Kültür University, Istanbul, Turkey; [b]Earthquake Engineering Department, Boğaziçi University, Kandilli Observatory and Earthquake Research Institute, Istanbul, Turkey; [c]Civil Engineering Department, Özyeğin University, Istanbul, Turkey

ABSTRACT

The reliability of V_{s30} and the performance of alternative time averaged shear wave velocities (V_{sz}) and shear wave travel times (T_{tz}) at various depths, z, were investigated for the estimation of site amplification and fundamental frequency (f_0) characterization by considering the linear and nonlinear soil behavior. The study revealed that alternative parameters performed better than V_{s30} and the best performing z parameters changed by switching from convex to concave theoretical profiles and by increasing ground motions. For a practical usage in site investigations, guidelines to estimate nonlinear soil amplification factor and fundamental frequency from the linear ones were presented.

ARTICLE HISTORY
Received 25 May 2023
Accepted 25 October 2023

KEYWORDS
Site amplification; fundamental soil frequency; nonlinear soil behavior; time averaged shear wave velocity; shear wave travel time; impedance ratio

1. Introduction

The seismic regulations on geotechnical and structural design require the consideration of site effects and soil amplification. Since the engineering practice needs fast and useful methods, time averaged shear wave velocity for the top 30 m, V_{s30}, has been the most commonly used and practical method for characterizing soil amplification. However, if two different soil profiles with the same V_{s30} values, but with different geologic units, number of horizontal soil layers, and depth to bedrock are considered, it is found that they do not alter the ground motion in the same way. Therefore, it is justified to further investigate the validity of V_{s30} for site amplification characterization in this study by constructing various shear wave velocity distributions. Also, a parametric investigation of alternative parameters, mainly averaged velocities and travel times at different depths (i.e. V_{sz} and T_{tz} at 5, 10, 20, 30, 40, 50, and 100 m), was performed for site amplification and fundamental frequency characterization by considering a layered soil media lying on elastic bedrock. Moreover, since the estimation of nonlinear soil amplification has always been a difficult issue, the possibility of predicting nonlinear soil amplification factor and nonlinear fundamental frequency from the linear ones was investigated, which can easily be identified from ambient ground noise measurements.

In seismic design codes such as the NEHRP Provisions (BSSC 1997), Uniform Building Code (ICBO 1997), Eurocode 8 (CEN 2004), and Turkish Building Seismic Code (TBSC 2018), the site classification method is based on V_{s30} due to its cost effectiveness and simplicity. Many researchers, however, stated that V_{s30} alone is not enough to reflect the properties of soil layers and proposed alternative and complimentary parameters. Steidl (2000) investigated the relation between V_{s30} and site amplification factors. The importance of depth-to-basement value was emphasized since the deeper sites showed higher site amplification factors. Stewart et al. (2003) mentioned that in long periods, neither V_{s30} nor detailed surface geology can correlate well with site amplification. Park and Hashash (2004) stated that site coefficients are highly dependent on the sediment thickness pointing out the insufficiency of V_{s30} for site classification. Mucciarelli and Gallipoli (2006) mentioned that

CONTACT N. Özge Fercan n.fercan@iku.edu.tr Civil Engineering Department, Istanbul Kültür University, Ataköy, Istanbul, Turkey

V_{s30} is not a good proxy of site amplification and the fundamental frequency, if the velocity profile is not increasing with depth monotonically and if there is not a strong impedance contrast in the velocity profile. Castellaro et al. (2008) reanalyzed the data set used by Boore (2004) and mentioned that site amplification is too complex to be defined with a single parameter. Lee and Trifunac (2010) stated that time averaged shear wave velocity is a weak proxy for site amplification. Regnier et al. (2011) suggested that V_{s30} alone does not represent soil stiffness accurately. Cadet et al. (2008) revealed that site parameters and site amplification factors are correlated well with fundamental frequency (f_0, V_{s30}) couple at most. Luzi et al. (2011) stated that the highest correlation with site amplification was achieved by (f_0, V_{s30}) couple, and as a single parameter f_0 performs better than V_{s30}. Similarly, Cadet et al. (2012) investigated the relation between site amplification, V_{sz} (i.e. z equal to 5, 10, 20, and 30 m) and the couples of (V_{sz}, f_0) alternative to V_{s30} and it was detected that the couple of (f_0, V_{s30}) shows the highest performance. Besides, as a single proxy for site amplification characterization, f_0 shows the highest correlation and provides lower misfits than V_{sz} parameters. Laurendeau et al. (2013) stated that site amplification depends on both V_{s30} and site Kappa, the high-frequency attenuation (κ_0). Zhao and Xu (2013) studied the correlation of site amplification ratios with V_{s30} and the parameter of site period (T_s, four times the shear-wave travel time from the bedrock to the ground surface) on a large ground-motion dataset (KiK-net data) which revealed T_s as a better proxy than V_{s30} for sites with T_s >0.6 s. Moreover, their performance was compared on ground motion prediction equations for site effect modelling, and T_s is defined as a better site parameter for all site classes again since it shows more reasonable median amplification ratios especially for soft soil sites at long spectral periods. Regnier et al. (2014) proposed a complimentary parameter to V_{s30}, B_{30} which is defined as the slope of V_s profile with depth and may help for the evaluation of site response. Hassani and Atkinson (2016) suggested replacing V_{s30} with f_0 in the ground-motion prediction equations. Derras et al. (2017) defined the best proxy as V_{s30} at short periods (T <0.6 s), while f_0 and H_{800} (where V_s is higher than 800 m/s) showed better performance at longer periods. Kwak and Seyhan (2020) studied the prediction of site effect parameter in ground motion modelling by capturing the shallow soil stiffness and impedance contrast by V_{s30} and deep sediment amplification by site fundamental period T_0 which characterizes the whole V_s profile down to bedrock. By using the V_s profiles and ground motion records of KiK-net database, this study focuses on the site effect modelling by investigating the performance of T_0 and deep sediment depth parameter (i.e. $z_{1.4}$=depth to V_s = 1.4 km/s) as a complementary to V_{s30}. They pick T_0 as the secondary site parameter which gives a better estimation. Also, these researchers revealed the nonlinear site effects by analyzing fundamental frequency shift and decrease in amplitude of soil amplification factor by gradually increasing ground motion intensities and implemented this finding as a nonlinear site effect model modification to linear site amplification model in ground motion models by empirical functions. Zhu et al. (2020) proposed site fundamental period (T_0) as the best performing single proxy and complementary to V_{s30}. Tsai et al. (2021) also stated that V_{s30} alone does not reflect the site effects if the site is not shallow and studied on a depth parameter (e.g. $Z_{1.0}$) which reflects deep site effects as a complementary parameter to V_{s30} for implementation in the seismic codes. They investigated the characterization of site factors at short and long periods obtained by both numerical 1D methods and empirical observations from the downhole arrays installed at Taipei basin for various bedrock depths. Hence, the study presents a depth correction factor which is derived with reference to the depth parameter (e.g. $Z_{1.0}$) for site factors obtained only by V_{s30}.

The previous studies interrogating the reliability of V_{s30} for site amplification and fundamental frequency characterization suggest using (V_{s30}, f_0) couples as the best performing parameter or some other alternative parameters related to depth, Kappa, soil profile, etc. Most of the studies investigated the performance of these correlations on the databases of seismically instrumented sites which enabled to use huge number of borehole logs including stiff to soft sites recorded various strong and weak motions by mostly analyzing the site amplification factors by response spectral ratios. Though the diversity of these soil profiles and the complex properties of recorded ground motions due to source, path, and site effects present realistic results for practice, the studies on these subjects repeat itself by means of methodology and suggested alternative parameters. As a novelty, in this study, theoretical shear wave velocity profiles distributed with depth in concave, linear, and convex shapes, were constructed to reveal if the optimal averaging depths of alternative parameters (i.e. V_{sz} and T_{tz}) correlating with site amplification ratio (i.e. maximum value in the surface-to-bedrock spectral ratio of Fourier amplitude spectra [FAS]) and fundamental frequency are changing by changing velocity distributions and by changing soil nonlinearity due to ground motion level. These constructed profiles were analyzed by considering two layering models for understanding the effect of layer number, layer thickness, and bedrock depth on soil response. A new parameter, T_{tz}, which can be obtained by geophysical field measurements, is proposed for the characterization of site amplification and fundamental frequency. In contrast to the studies just analyzed linear soil behavior by weak motions and proposed V_{sz} parameters for linear site amplification characterization (i.e. Cadet et al. 2012; Regnier et al. 2011), the nonlinear soil behavior is considered as well by gradually increasing bedrock accelerations in this study; hence, the proposed best correlating V_{sz} and T_{tz} parameters with soil amplification and fundamental frequency, represent both linear and nonlinear soil behavior. This study includes a detailed investigation of linear to nonlinear soil response which is figured out by analyzing the transfer functions of soils (i.e. surface-to-bedrock ratio of the FAS), modulus degradation, shear strains, and surface PGAs. Moreover, guidelines were constituted as a practical method for the estimation of nonlinear fundamental frequency and soil amplification from the linear ones which can be easily calculated by field measurements.

2. Soil Models of Equal Thickness and Equal Travel Time for Each Layer

In this study, 17 shear wave velocity profiles were constructed for the bedrock depth of 100 m, changing from convex (i.e. the velocities changing faster near the surface and slower near the bedrock) to concave (i.e. the velocities changing slower near the surface and faster near the bedrock). For analysis, the soil media was divided into layers, first with equal thickness, and then with equal wave travel times. It was intended to observe the effect of layering type (i.e. equal thickness, and equal wave travel times) on soil response, hence soil response characterizing parameters.

The soil model with equal layer thickness has 50 layers and the thickness of each layer is defined as 2 m. All shear wave velocity profiles begin with $V_s = 50$ m/s at the first layer ending with $V_s = 1000$ m/s at the last layer which overlies an elastic bedrock with $V_s = 2000$ m/s. The shear wave velocity profiles were divided into three groups according to the geometric shapes of them as concave, linear, and convex (Fig. 1). For the concave profile, the velocities increase slower near the surface and faster near the bedrock, whereas for the convex profile, the velocities increase faster near the surface and slower

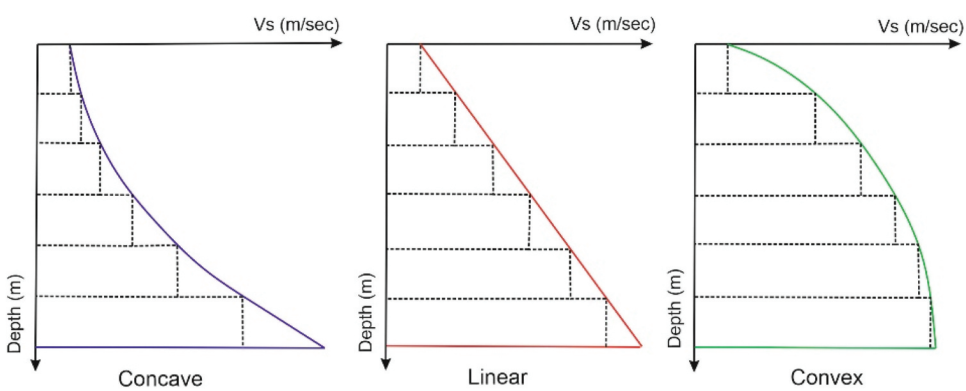

Figure 1. Geometric shapes of concave, linear, and convex type shear wave velocity profiles.

near the bedrock. The linear profile represents the transition from concave to convex. Among the shear wave velocity profiles used, ten are concave type, one is linear type, and six are convex type.

In order to investigate the variation of soil amplification for softer profiles in more detail, higher number of concave profiles was used. The profiles are numbered from 1 to 10 representing decreasing stiffness for concave type and 1 to 6 representing increasing stiffness for convex type (Fig. 2a). The velocities increase rapidly near the surface as the soil profile turns from concave to convex. Therefore, Convex-6 type profile shows a higher stiffness than Concave-10.

The velocity profiles were generated by using a single equation by changing the coefficients of a and c and constant of n;

$$v_i = \left[\frac{i-n}{a}\right]^{1/c} \tag{1}$$

in which v_i represents mean shear wave velocity of each soil layer, and i represents the layer number from the surface. The values of coefficients a and c, and the constant n are given in Table 1.

For the soil model with equal wave travel time, the number of layers and the bedrock depths vary according to each velocity profile. The equal travel time of each layer is defined as 0.04 s, since it corresponds to the lowest V_s and layer thickness, 50 m/s (i.e. for the first layer)

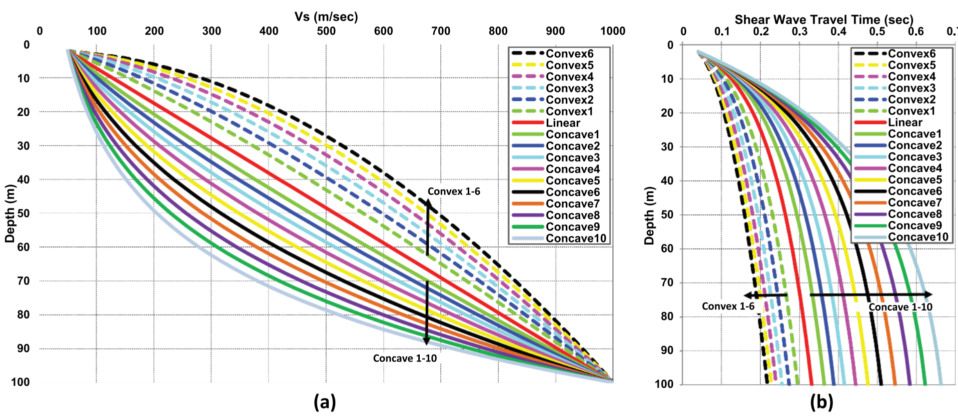

Figure 2. a Shear wave velocity profiles changing from concave to convex (i.e. from left to right) for equal layer thickness model; (b) incremental shear wave travel times for the velocity profiles of equal layer thickness model.

Table 1. Coefficients and constants of general equation for soil profiles.

Soil Profile Type	*a*	*n*	*c*
Convex-1	0.01270	−0.38	1.20
Convex-2	0.00445	0.12	1.35
Convex-3	0.00157	0.44	1.50
Convex-4	0.00055	0.64	1.65
Convex-5	0.00019	0.77	1.80
Convex-6	0.00006	0.85	1.95
Linear	0.05158	−1.57	1.00
Concave-1	0.14984	−3.16	0.85
Concave-2	0.30812	−4.79	0.75
Concave-3	0.64128	−7.15	0.65
Concave-4	1.35848	−10.6	0.55
Concave-5	2.95672	−16.2	0.45
Concave-6	6.72342	−25.4	0.35
Concave-7	16.5302	−42.9	0.25
Concave-8	48.0320	−85.3	0.15
Concave-9	249.369	−302.2	0.05
Concave-10	−428.342	353.2	−0.05

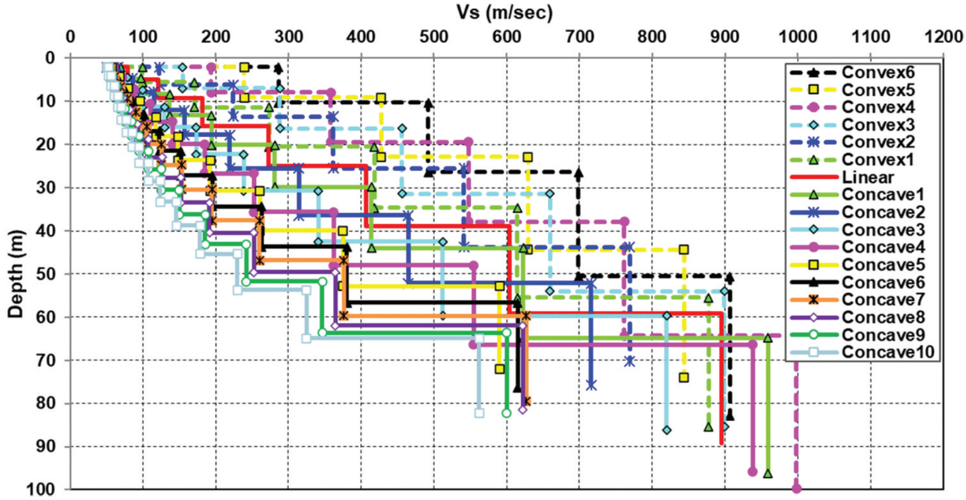

Figure 3. Soil profiles with equal shear wave travel time ($t = 0.04$ s) for each layer.

and 2 m, respectively. The layer thickness of equal wave travel time model was obtained by using the velocity profiles of equal layer thickness model. First, incremental wave travel times were calculated for each velocity profile (Fig. 2b), and the depth of each layer was extracted, corresponding to a wave travel time of 0.04 s. Shear wave velocities corresponding to the identified depths were obtained by using the velocity profiles of equal layer thickness model by Fig. 2a.

Then, the soil profiles with equal wave travel times (i.e. 0.04 s for each layer) changing from concave to convex were obtained (Fig. 3). In Fig. 3, the top layer of all profiles has $V_s = 50$ m/s, and the layer thickness increases near the bedrock as the wave velocity increases with depth. The thicknesses of the soil layers are different for all profiles, because of the requirement of equal wave travel times in each layer. It was aimed to observe the dynamic soil response due to these two layering models: first by holding layer thickness, layer number, and bedrock depth constant and then holding wave travel times constant for each layer leading to variation in layer thickness, layer number, and bedrock depth.

3. Impulsive and White-Noise Bedrock Motions

Soils behave linearly or nonlinearly due to the amplitude level and frequency content of the ground motion which causes a variation in soil amplification factors, and the fundamental frequencies. To investigate this variation independent from the source, path, directivity effects, and instrument distortions leading to complex properties in earthquake records (i.e. amplitude, frequency content, and duration), impulsive, and white-noise motions were used for the analyses. They are considered as the boundaries of variations in the frequency content and amplitude of bedrock motions. The impulsive bedrock motion is modeled as a Delta function which gives constant Fourier amplitudes for all frequencies. The PGA levels of the impulsive bedrock accelerations varied between 0.005*g* and 1.0*g* (Fig. 4a).

The second type of bedrock motion used for the analysis is zero-mean Gaussian white-noise with PGA values varying from 0.005*g* to 1.0*g* (Fig. 5a). The sampling rate of the simulated impulsive and white-noise bedrock accelerations is 200 sps, corresponding to a Nyquist frequency of 100 Hz. The wide and random range of frequency content of white-noise presents higher Fourier amplitudes than the impulsive motions have, even if they have the same PGA level (Fig. 4b and 5b)

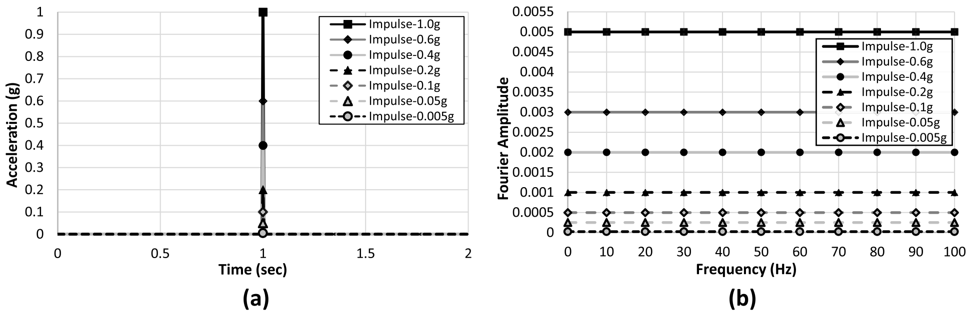

Figure 4. Impulsive accelerations with different amplitudes (gradually increasing PGAs: 0.005*g*, 0.05*g*, 0.1*g*, 0.2*g*, 0.4*g*, 0.6*g*, and 1.0*g*): (a) acceleration–time history; (b) Fourier amplitude spectra.

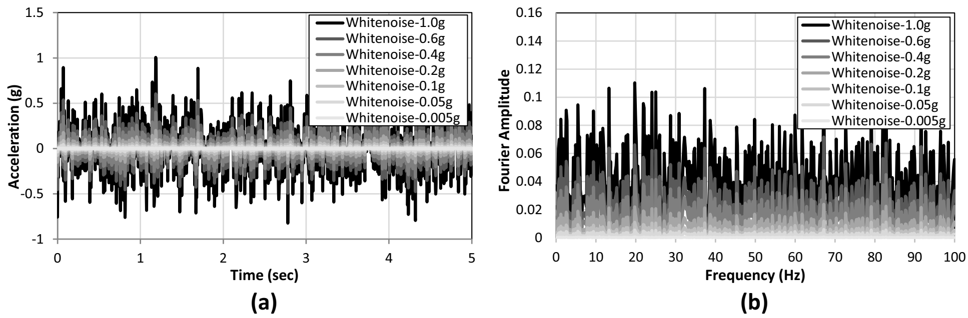

Figure 5. White-noise motions with gradually increasing PGAs: (a) acceleration–time history; (b) Fourier amplitude spectrum.

4. Soil Properties for Site Response Analysis

Site response of each soil profile was computed by both linear and equivalent-linear analyses for the given bedrock motions by using DEEPSOIL (Hashash et al. 2008). The site amplification factors and fundamental frequencies were obtained for each soil profile and layering method (i.e. equal thickness and equal travel time) by gradually increasing bedrock accelerations.

In DEEPSOIL, the initial shear modulus (i.e. G_{max}) is computed from the shear wave velocity and the density, ρ, by the equation of $V_s=\sqrt{G_{max}/\rho}$ automatically. For equivalent-linear analysis, which is an approximation of a nonlinear model, the unit weight and initial damping ratio of each layer above the bedrock were assigned as $\gamma = 18$ kN/m^3 and $\xi = 0.48\%$ respectively. For the bedrock, the following properties were assigned; $V_s = 2000$ m/s, $\gamma = 22$ kN/m^3 and $\xi = 2\%$. Equivalent-linear model requires the determination of modulus reduction and damping ratio curves at discrete points since the method chooses appropriate shear modulus and damping ratio value corresponding to induced strains due to soil response by an iterative procedure. For the whole soil profile, the soil modelling parameters were kept constant to observe the soil response just by changing velocity profiles. The same modulus reduction, $G/G_{\max}$, and damping ratio curve of Seed and Idriss (1970) were used for all soil layers (Fig. 6). Seed and Idriss (1970) suggest three types of curves for sands, based on their stiffness. It was chosen as "mean sand," which presents a moderate stiffness and damping ratio.

5. Site Amplification Characterization Parameters

The averaged shear wave velocities, V_{sz}, and the shear wave travel times, T_{tz}, for different depths, z, were calculated to investigate the correlation with site amplification factors and fundamental frequencies. V_{sz} was defined for $z = 5$, 10, 20, 30, 40, 50, and 100 m by the following equation:

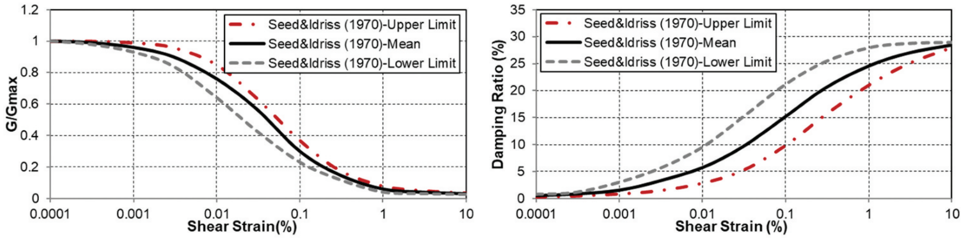

Figure 6. G/G_{max}, and damping ratio curves of Seed and Idriss (1970) with respect to shear strains, γ_c.

$$V_{sz} = \frac{\sum h_i}{\sum\left(\frac{h_i}{V_{si}}\right)} \tag{2}$$

where h_i is the thickness of the i'th layer. It is clear that V_{sz} is indirectly related to the shear wave travel time, as it is seen by the term in the denominator of the equation. Shear wave travel times were generated for 5, 10, 20, 30, 40, 50, and 100 m by the following equation:

$$T_{tz} = \sum \frac{h_i}{V_{si}} \tag{3}$$

Shear wave travel time at a specific depth, z, is obtained by the sum of wave travel times [i.e., (*sum of the layer thickness/shear wave velocity* ratios)]. V_{sz} and T_{tz} are presented in Tables 2 and 3 for equal layer thickness model. As the velocity profiles change from concave to convex, the stiffness of soil increases, and the wave travel times decrease due to increasing wave velocity. V_{s100} and T_{t100} reflect the averaged shear wave velocity and wave travel time for the bedrock depth 100 m, respectively.

6. Evaluation Method of Site Amplification and Fundamental Frequency Characterization Parameters

Soil response in this numerical study was evaluated by soil amplification factors and fundamental frequencies that were obtained from the surface-to-bedrock transfer functions. In this study, the soil amplification factor, AF, is defined as the maximum value in the surface-to-bedrock spectral ratio of FAS and the corresponding frequency as the fundamental frequency, f_0. Although it is not presented in the paper, we have also checked the ratios of secondary peaks, as well as the ratio of the average

Table 2. V_{sz} of the soil profiles with equal layer thickness.

Profile No.	Soil Type	V_{s05} (m/s)	V_{s10} (m/s)	V_{s20} (m/s)	V_{s30} (m/s)	V_{s40} (m/s)	V_{s50} (m/s)	V_{s100} (m/s)
1	Convex-6	85	127	188	236	277	314	459
2	Convex-5	82	120	177	222	261	297	439
3	Convex-4	78	112	165	207	244	278	416
4	Convex-3	74	104	152	191	226	258	392
5	Convex-2	70	96	139	175	207	237	366
6	Convex-1	67	89	126	159	189	217	338
7	Linear	62	80	111	139	165	190	302
8	Concave-1	60	74	100	125	148	170	275
9	Concave-2	58	70	94	116	138	159	258
10	Concave-3	57	67	88	108	128	147	241
11	Concave-4	56	65	83	101	119	137	225
12	Concave-5	55	63	79	95	111	127	210
13	Concave-6	54	61	75	89	104	119	196
14	Concave-7	54	59	71	84	97	111	183
15	Concave-8	53	58	68	80	91	104	171
16	Concave-9	53	57	66	76	86	98	161
17	Concave-10	52	56	64	73	82	92	151

Table 3. T_{tz} of the soil profiles with equal layer thickness.

Profile No.	Soil Type	T_{t05} (s)	T_{t10} (s)	T_{t20} (s)	T_{t30} (s)	T_{t40} (s)	T_{t50} (s)	T_{t100} (s)
1	Convex-6	0.059	0.079	0.106	0.127	0.144	0.159	0.218
2	Convex-5	0.061	0.084	0.113	0.135	0.153	0.169	0.228
3	Convex-4	0.064	0.089	0.122	0.145	0.164	0.180	0.240
4	Convex-3	0.067	0.096	0.132	0.157	0.177	0.194	0.255
5	Convex-2	0.071	0.104	0.144	0.171	0.193	0.211	0.274
6	Convex-1	0.075	0.113	0.158	0.189	0.212	0.231	0.295
7	Linear	0.080	0.126	0.181	0.216	0.243	0.264	0.331
8	Concave-1	0.084	0.136	0.200	0.241	0.270	0.293	0.364
9	Concave-2	0.086	0.142	0.213	0.258	0.291	0.315	0.388
10	Concave-3	0.088	0.148	0.227	0.277	0.313	0.339	0.415
11	Concave-4	0.089	0.154	0.241	0.297	0.336	0.365	0.444
12	Concave-5	0.091	0.160	0.254	0.317	0.360	0.393	0.476
13	Concave-6	0.092	0.165	0.268	0.337	0.386	0.421	0.510
14	Concave-7	0.093	0.169	0.281	0.357	0.412	0.451	0.545
15	Concave-8	0.094	0.173	0.292	0.377	0.438	0.482	0.583
16	Concave-9	0.095	0.176	0.303	0.396	0.463	0.513	0.623
17	Concave-10	0.096	0.179	0.313	0.414	0.488	0.544	0.663

spectral amplitudes over a narrow frequency band centered at the fundamental frequency. The amplitudes were sometimes different, but the input-to-output ratios were not much different both for the convex and concave profiles. We chose the peak spectral ratio amplitudes as the site amplification value both for its simplicity and for mostly representing an upper bound. The optimal (i.e. those with the highest correlations) V_{sz} and T_{tz} parameters for site amplification have been decided by plotting AF/V_{sz} [or, (AF/T_{tz})] values for each velocity profile and finding the one that is closest to a horizontal straight line [i.e. the mean of data set (AF/V_{sz})] (Fig. 7).

The optimal V_{sz} and T_{tz} parameters for fundamental frequency has been decided by plotting f_0/V_{sz} [or, $(f_0 x T_{tz})$] values for each velocity profile and finding the one that is closest to a horizontal straight line [i.e. the mean of data set (f_0/V_{sz})].

To quantify the performance of the parameters used, a two-stage methodology was followed. First, the mean absolute error (MAE) of each data set [e.g. (AF/V_{sz})] with respect to the mean value of the data set was obtained for linear/concave and convex profiles separately. The mean error of each data set was scored by the following equation:

$$MAE = \min_{Z}\left[\frac{1}{n}\sum\nolimits_{i=1}^{n}|y-\hat{y}|_i\right] \quad (4)$$

where y equals to data point among the data set, $\hat{y}$ equals to mean of the data set, n equals to the number of data points in the data set and z represents each performing parameter. The smaller MAE

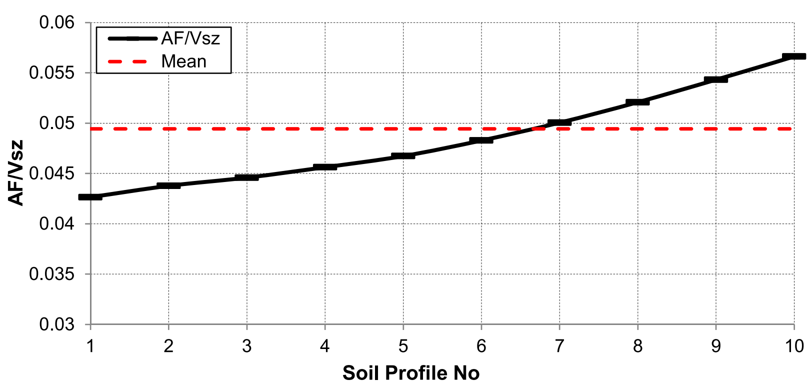

Figure 7. AF/V_{sz} data set and the mean of the data set as the best fitting straight line.

score represents the higher correlation with the relevant soil characterization parameter for each group of soil profiles (e.g. convex profiles). After deciding the mean best performing z value (i.e. V_{sz}, T_{tz}) for each profile group by the lowest *MAE*, the best performing *z* value should be defined for each specific profile among the group as well by absolute error (*AE*).

The *AE* of each parameter was calculated for each profile with respect to the mean value of the parameter. The error is quantified as the spread of the parameter around the mean by the following equation:

$$AE = \min_{Z} |y - \hat{y}| \tag{5}$$

where *y* equals to data point among the data set, $\hat{y}$ equals to mean of the data set and *z* represents each performing parameter. The level of *AE* value denotes the correlation term; the smaller the *AE* the higher the correlation for the soil response characterization. By this equation, *AE*s are calculated for each *z* value (i.e. V_{sz}, T_{tz}) and the minimum value of *AE* revealing best performing parameter (e.g. V_{s05}, V_{s10}, V_{s20}, etc.) is chosen for each profile. The *AE*s for the convex and linear/concave velocity profiles were presented separately for each bedrock acceleration level. However, the best performing parameter should be defined by considering both *MAE* score of AF/V_{sz} [or (AF/T_{tz}), (f_0/V_{sz}) and $(f_0 \times T_{tz})$] correlations and *AE* graphs.

7. Site Response Analyses

Linear and nonlinear soil response for the constructed soil profiles were presented by explaining the transfer functions of soils. First, linear analyses were carried out for equal layer thickness model by using an impulse at the bedrock level with PGA amplitudes 0.1*g*, 0.4*g*, and 1.0*g*. Since the soil model is linear, the soil amplification factors, and fundamental frequencies were the same for all bedrock acceleration levels. Also, *AF* and f_0 were observed nearly the same as those obtained by equivalent-linear analysis for 0.005*g* impulsive bedrock acceleration level. Thereby, for the profiles given, linear site response analysis is only applicable for low bedrock accelerations inducing linear soil behavior (Acc.$\leq$0.005*g*).

Equivalent-linear approach was used for each layering type and velocity profile by using impulsive and white-noise bedrock accelerations. The approach is suitable for calculating linear and nonlinear site response for a broad range of strain rates. The site response analyses were carried out by equivalent-linear model for the following combinations: 1. Equal layer thickness (i.e. "$h = 2$ m") model by impulsive accelerations (i.e. "I"); 2. Equal layer thickness (i.e. "$h = 2$ m") model by white-noise accelerations (i.e. "W"); 3. Equal wave travel time (i.e. "$t = 0.04$ s") model by impulsive accelerations (i.e. "I").

The surface-to-bedrock transfer functions were studied for gradually increasing bedrock acceleration levels to obtain soil amplification factors and fundamental frequencies. The transfer functions were computed as the surface-to-bedrock ratio of the FAS of accelerations. In Fig. 8, the variation of transfer functions is shown for increasing impulsive bedrock acceleration levels from 0.005*g* to 1.0*g* for equal layer thickness model (i.e. $h = 2$ m). The maximum values of the FAS ratios (i.e. the soil amplification factor, *AF*; *y*-axis) are marked by circles on the figures. The following observations were revealed:

(1) The transfer functions at 0.005*g* impulse level were the same as those for linear analysis. The shear strains were in linear elastic range (0.001% < γ); hence, the stiffness of profiles did not change (G/G_{max} >0.96) at 0.005*g* impulse level.
(2) A sharp difference was observed between convex and linear/concave profiles in soil amplification behavior. The soil amplification factors (i.e. *AF*, the maximum amplitudes here) were obtained approximately in the range of 11–22 for 0.005*g* impulse type bedrock acceleration level and 5–9 for 1.0*g* impulse type bedrock acceleration level by the variation of soil profiles. This much higher soil

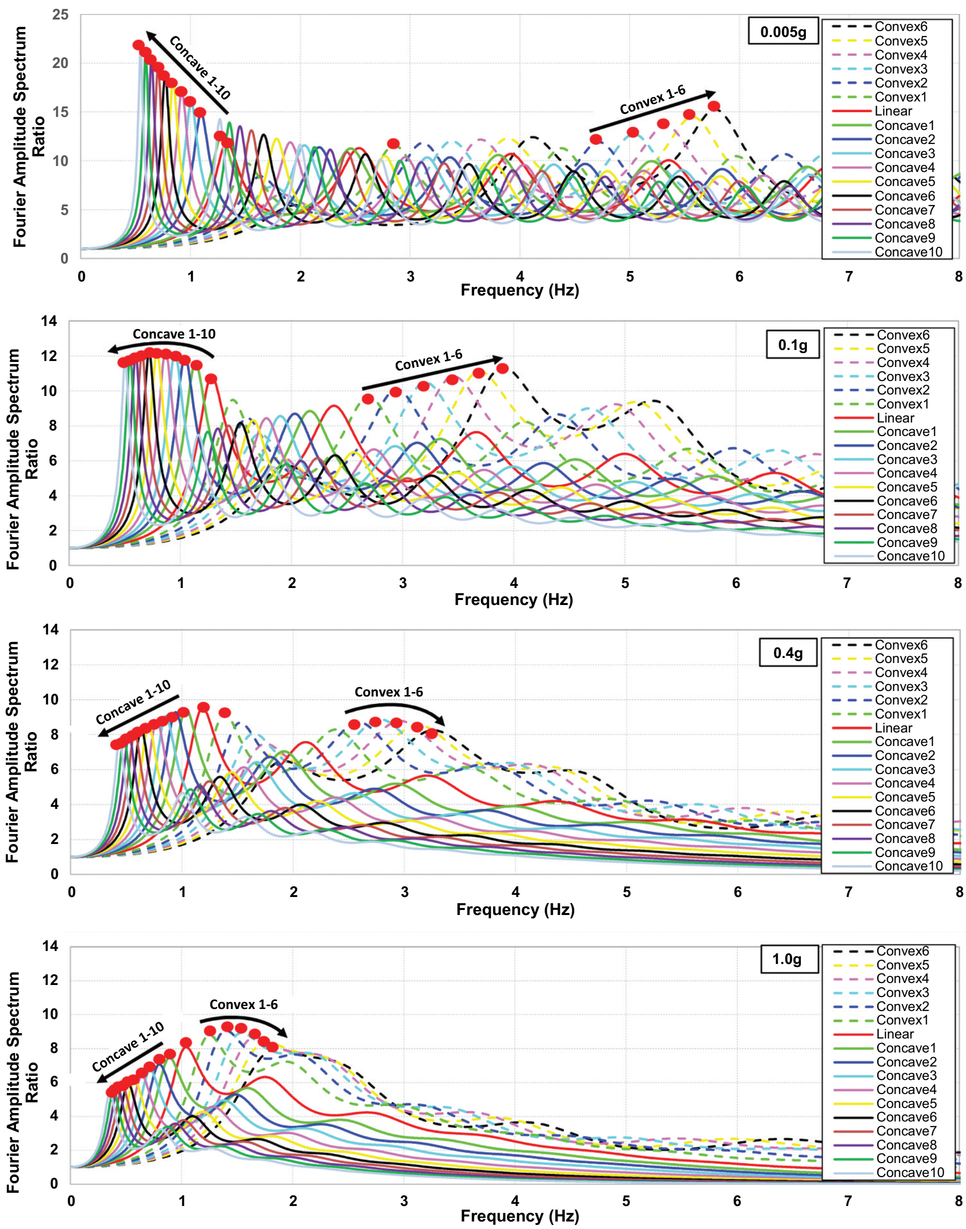

Figure 8. Transfer functions for $h = 2$ m model for increasing impulsive bedrock acceleration levels.

amplification factors at lower bedrock acceleration levels can be explained by the linear behavior of soil which induced very small stiffness degradation and hence lower damping ratio. As the bedrock acceleration level increased, the soil amplification level decreased due to increasing modulus reduction and damping ratio for all profiles. At perfectly linear elastic strain range (i.e. 0.005*g* bedrock acceleration level here), the softer velocity profiles presented higher soil amplifications than stiffer velocity profiles, and vice versa at perfectly elasto-plastic strain range (i.e. 1.0*g* bedrock acceleration level here).

(3) Nonlinear soil response developed more rapidly for linear and concave type (i.e. E soil class according to NEHRP (National Earthquake Hazards Reduction Program 1997), V_{s30} <180 m/s)

soil profiles by decreasing soil amplification factors, deamplified surface PGAs, and observed maximum shear strains in the soil layers. Lower stiffness of these profiles induced higher and faster modulus degradation compared to the convex type profiles (i.e. D soil class according to NEHRP, 180< V_{s30} <360 m/s), resulting in lower surface PGAs and higher surface displacements as a soft soil seismic demand.

(4) The effect of soil stiffness and the impedance contrast between layers were tested by this study. The linear and concave profiles were pronounced as softer soils compared to stiffer convex profiles. As the profiles changed from concave to convex, rapid increase of the velocities near surface caused higher impedance constrast (i.e. low impedance ratio) on the top layers (Table 4). For convex profiles, even if the shear wave velocities are high on top layers, low impedance ratio caused amplification of surface PGAs. According to the theory of the soil response of uniform damped or undamped soil layer on the elastic rock due to ground motion excitation by Kramer (1996), the amplitude of the soil amplification factor is inversely proportional with the impedance ratio; the lower the impedance ratio, the higher the soil amplification level. As compatible with this theory, this study showed the amplification of surface PGAs in stiffer profiles which is caused by high impedance contrast mainly. In contrast to the soft soil amplification concept, stiff soil amplification was observed as it is revealed in the previous studies focused on seismically instrumented sites as well (Andreotti and Calvi 2021; Calvi and Andreotti 2022; Mucciarelli and Gallipoli 2006; Xiao et al. 2022).

(5) Due to lower soil stiffness, fundamental frequencies of concave type profiles were observed less than the fundamental frequencies of convex profiles. Moreover, as the nonlinearity increased, the f_0 decreased for all profiles due to the fact that $V_s \propto \sqrt{G_{sec}/\rho}$ which is stated as the fundamental frequency shift in the studies of Regnier et al. (2013) and Kwak and Seyhan (2020) as well. High-order f_0 peaks (second and third) of convex profiles were shifted to the first order by gradually increasing bedrock accelerations. Because, high frequency spectral amplitudes of convex profiles were damped by increased stiffness degradation at the top layers due to high amplitude shear stress transfer from bedrock.

(6) It has been detected that the fast transition from high impedance ratio (α_z) to low impedance ratio (i.e. high impedance contrast) at thin layers (i.e. 2 m here) near surface caused high-order f_0 peaks in convex profiles (Table 4).

The trends of transfer functions for the other combinations of layering and bedrock acceleration types were detected nearly the same as the presented combination (i.e. $h = 2$ m, I) except the range of the soil amplification factors and fundamental frequencies. The same velocity profiles with different layering discretization (i.e. $t = 0.04$ s) resulted in closer cyclic behavior of soil, which reveals that different layer number, layer thickness and bedrock depth do not make a big difference in the site amplification behavior of soils if the wave travel time of each layer is the same, corresponding to the same velocity distribution with $h = 2$ m model (Table 5).

Table 4. Impedance ratio and shear wave velocities for $h = 2$ m model.

	Concave-10		Linear		Convex-6	
Layer No.	V_s (m/s)	α_z	V_s (m/s)	α_z	V_s (m/s)	α_z
1	50.0	0.9447	50.0	0.721	50.0	0.3441
2	52.9	0.9446	69.4	0.782	145.3	0.7244
3	56.0	0.9444	88.8	0.821	200.6	0.8217
4	59.3	0.9443	108.2	0.848	244.1	0.8679
–						
48	876.8	0.9365	961.2	0.980	978.9	0.9893
49	936.3	0.9363	980.6	0.981	989.5	0.9895
50	1000	0.5000	1000	0.500	1000	0.5000

Table 5. Impedance ratio and shear wave velocities of $t = 0.04$ s model.

	Concave-10			Linear			Convex-6		
Layer No.	V_s (m/s)	Depth (m)	α_z	V_s (m/s)	Depth (m)	α_z	V_s (m/s)	Depth (m)	α_z
1	50.0	2.0	0.941	50.0	2.0	0.633	50.0	2.0	0.175
2	53.1	4.1	0.937	79.0	5.0	0.654	286.3	10.3	0.582
3	56.7	6.4	0.933	120.7	9.3	0.662	492.2	26.4	0.705
4	60.7	8.8	0.928	182.2	15.6	0.667	698.6	50.5	0.770
5	65.4	11.4	0.923	273.2	25.0	0.671	906.6	82.9	0.453
6	70.9	14.2	0.915	407.1	38.8	0.673	–		
7	77.5	17.2	0.907	604.4	59.2	0.675			
8	85.4	20.6	0.897	895.2	89.2	0.448			
9	95.2	24.3	0.885	–					
10	107.6	28.5	0.869						
11	123.8	33.2	0.848						
12	146.0	38.7	0.819						
13	178.3	45.4	0.777						
14	229.6	53.7	0.707						
15	324.7	64.9	0.578						
16	562.3	82.3	0.281						

7.1. Site Amplification Characterization by Surface PGA

The correlations between soil amplification factors and surface PGAs were investigated by the ratio of *AF* to surface PGAs for increasing bedrock accelerations and different layering schemes (Fig. 9). The surface PGAs were amplified and soil amplification factors were observed higher for 0.005*g* bedrock acceleration level than those for higher bedrock accelerations by the effect of linearity. Since the amplified surface PGAs were in quite lower ranges (i.e. 0.0071*g*–0.0105*g*), the ratio of soil amplification factors to surface PGAs was observed higher for 0.005*g* bedrock acceleration level. Besides, the surface PGAs were found to be higher for convex types (i.e. profile no. 1 to 6) than the concave types (i.e. profile no. 8 to 17) due to low impedance ratio between top layers, though the stiffness of layers was high along the profile for convex types. Soil amplification characterization by surface PGAs was studied for each layering (i.e. $h = 2$ m and $t = 0.04$ s) and bedrock motion type (i.e. I and W). It is determined that the surface PGA can characterize soil amplification only for convex profiles for bedrock acceleration levels $\geq$0.1*g* (i.e. nonlinear elastic and elasto-plastic strain range) based on lower *MAE* values for all layering and bedrock acceleration types (Table 6). The *MAE* values lower than 4.5 present a correlation for soil amplification

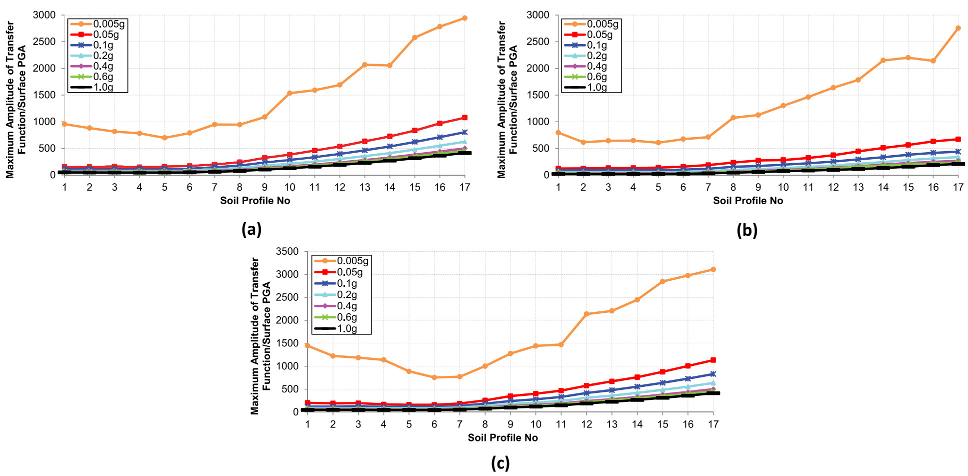

Figure 9. The correlation of AF with surface PGAs: (a) $h = 2$ m, I; (b) $h = 2$ m, W; (c) $t = 0.04$ s, I.

Table 6. MAE values for the correlation of AF/surface PGA for convex profiles.

Bedrock PGA	$h = 2$ m, I	$h = 2$ m, W	$t = 0.04$ s, I
0.005g	65.3	47.1	189.6
0.05g	5.4	9.1	16.7
0.1g	2.5	4.4	3.9
0.2g	2.2	2.0	2.0
0.4g	1.4	2.2	1.9
0.6g	1.6	1.8	1.7
1.0g	1.2	1.3	1.3

Note: I= impulsive motion; W= white-noise motion; "$h = 2$ m" = equal layer thickness model; "$t = 0.04$ s" = equal wave travel time model.

factor and surface PGA. For concave and linear profiles, there is not a constant ratio between the amplification factor and the surface PGA.

7.2. Site Amplification Characterization by Fundamental Soil Frequency, f_0

The correlation between soil amplification factors and fundamental frequencies was investigated by the ratio (soil amplification/fundamental frequency) with profile numbers (Fig. 10). A constant ratio was observed between these parameters at linear elastic and nonlinear elastic strain range triggered by the acceleration levels below 0.4g for convex profiles. f_0 performed well only for convex profiles for Acc.$\leq$0.4g based on MAE score $\leq$1.2 for each layering and bedrock acceleration type.

7.3. Site Amplification Characterization by V_{sz}

The correlation of soil amplification factors with time averaged shear wave velocities at various depths, V_{sz}, was investigated by checking both if AF/V_{sz} ratios were close to a constant due to MAE score close to 0 and by checking the lowest AE values to decide on the best performing z parameter. AF/V_{sz} ratios were presented for $h = 2$ m, I model (Fig. 11). At 0.005g and 0.1g bedrock acceleration levels, all AF/V_{sz} ratios showed nearly constant lines and hence low MAE score < 0.007 for convex profiles, while there was not any correlation for linear and concave profiles (Fig. 12). As the nonlinearity increased by 0.2g, 0.4g, 0.6g, and then 1.0g bedrock accelerations, the constant ratio between AF and V_{sz} for convex profiles deteriorated for the shallow averaging depths indicated by high MAE scores, while V_{sz} presented a better performance of site amplification characterization for linear and concave profiles.

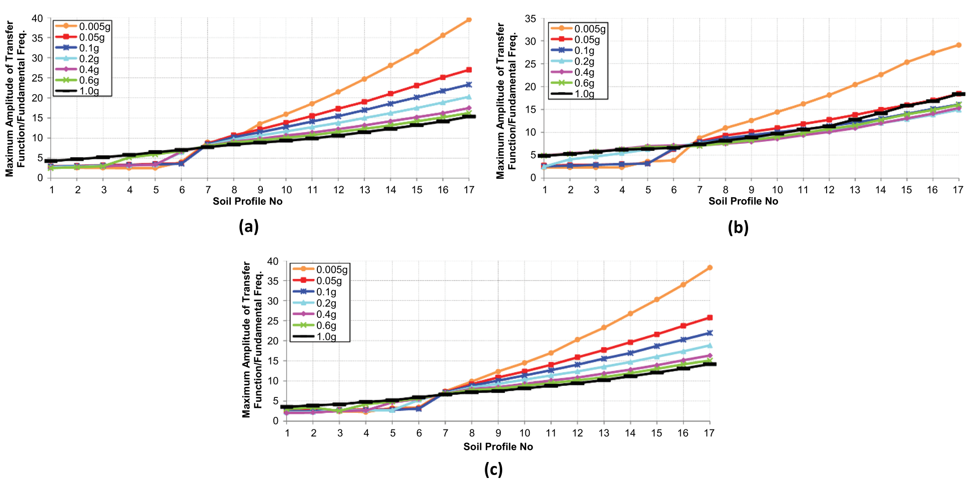

Figure 10. The correlation of AF with f_0: (a) $h = 2$ m, I; (b) $h = 2$ m, W; (c) $t = 0.04$ s, I.

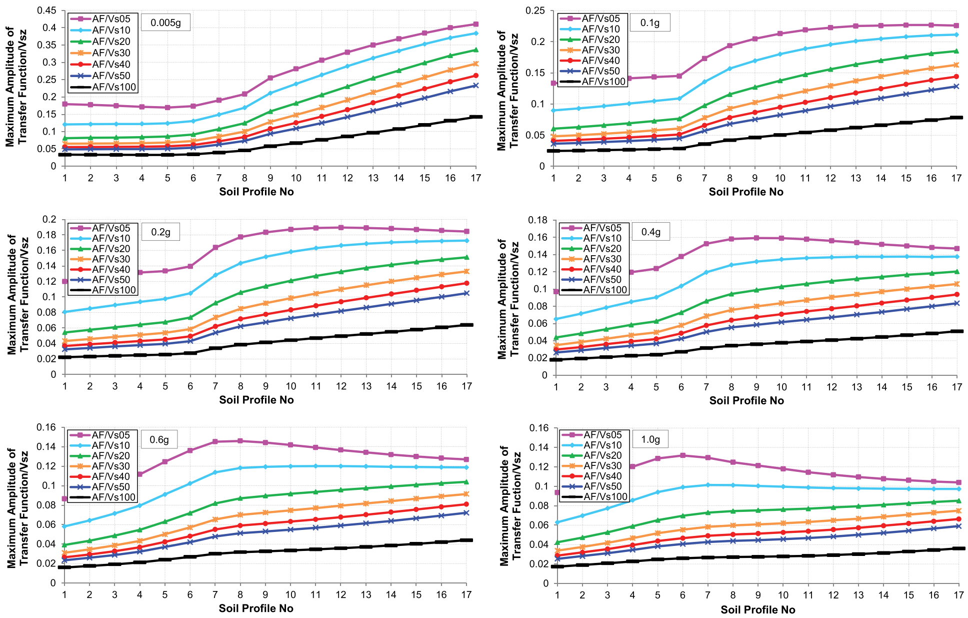

Figure 11. The correlation of AF with V_{sz} for $h = 2$ m, I model.

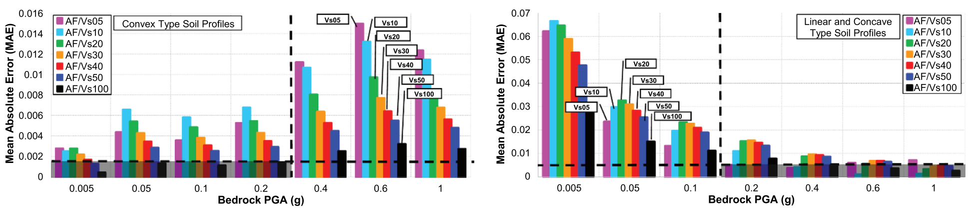

Figure 12. *MAE* values for the correlation of *AF* with V_{sz} for $h = 2$ m, I model; the best performing V_{sz} parameters were labeled in the graph from left to right by an increasing *z* order.

In Fig. 12, the shaded area presents the lowest *MAE* values pointing out the best performing *z* parameter for each profile group due to increasing bedrock acceleration levels and the dashed vertical line presents the threshold level of bedrock accelerations for the validity of a correlation.

The *AE* performance levels (i.e. scattering level from a horizontal straight line) with respect to increasing impulsive bedrock PGAs are shown for convex and linear/concave profiles in Fig. 13. Linear and concave profiles presented lower *AE* at 0.2*g*, 0.4*g*, 0.6*g*, and 1.0*g* bedrock accelerations leading to a good V_{sz} performance for soil amplification characterization at nonlinear elastic and elasto-plastic

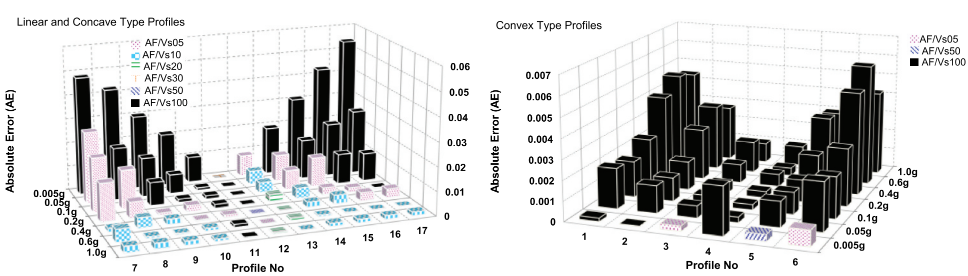

Figure 13. The variation of *AE* for AF/V_{sz} for $h = 2$ m, I model.

Table 7. The best performing V_{sz} parameters for soil amplification characterization.

	AF/V_{sz}					
Profile Type	Linear/Concave			Convex		
Bedrock PGA	$h = 2$ m, I	$h = 2$ m, W	$t = 0.04$ s, I	$h = 2$ m, I	$h = 2$ m, W	$t = 0.04$ s, I
0.005g	–	–	–	V_{s100} or V_{s50}	V_{s100} or V_{s50}	V_{s50}
0.05g	–	V_{s05}	–	V_{s100} or V_{s50}	V_{s100} or V_{s50}	V_{s50}
0.1g	–	V_{s10}	–	V_{s100} or V_{s50}	V_{s100} or V_{s50}	V_{s50}
0.2g	V_{s05}	V_{s10}	V_{s05}	V_{s100} or V_{s50}	V_{s100} or V_{s50}	V_{s50} or V_{sz}
0.4g	V_{s10} or V_{s05}	V_{s10}	V_{s05}	–	V_{s100} or V_{s50}	–
0.6g	V_{s10}	V_{s10}	V_{s10}	–	V_{s100} or V_{s50}	–
1.0g	V_{s10}	V_{s10}	V_{s10}	–	V_{s100} or V_{s50}	–

Note: AF=soil amplification factor; V_{sz}= averaged shear wave velocity at depth z; I= impulsive motion; W= white-noise motion; "$h = 2$ m"= equal layer thickness model; "$t = 0.04$ s"= equal wave travel time model.

strain ranges. V_{s100} had the best performance for all convex profiles at bedrock accelerations > 0.005g. This finding supports the study by Luzi et al. (2011) in which the best performing parameter representing the complete impedance contrast for the whole soil profile is the V_{s100} parameter, averaged wave velocity depth to bedrock. However, since it is hard to obtain and impractical to use V_{s100}, the averaged shear wave velocity at 100 m which is depth to bedrock, V_{s50} can be used instead which is the next best performing parameter after V_{s100} as it is presented by *MAE* score in Fig. 12. Based on the same evaluation method, the optimal V_{sz} parameters for the characterization of soil amplification factors are presented in Table 7.

According to Table 7, the optimal V_{sz} parameters are:

- For linear and concave profiles: V_{s10} or V_{s05} for impulsive Acc.≥0.2g and white-noise Acc.≥0.05g.
- For convex profiles: V_{s100} or V_{s50} for impulsive Acc.≤0.2g and for all white-noise accelerations. The performance of different V_{sz} parameters is changing due to nonlinearity of the soil profiles for increasing bedrock accelerations which vary in frequency content. Here, the correlations and the best performing parameters for the model $t = 0.04$ s were observed similar with the ones for $h = 2$ m model. Besides, the correlations for white-noise motions were observed for a wider range of bedrock accelerations. However, for a conservative and inclusive approach in practice, V_{s10} is more reflective of the soil profile than V_{s05}; hence, it can be used for the ground accelerations ≥0.2g for linear and concave type soil profiles and V_{s50} can be used for the ground accelerations ≤0.2g for convex profiles.

7.4. Site Amplification Characterization by T_{tz}

Alternative to V_{sz}, the wave travel times were investigated for various depths, T_{tz}, as a parameter to characterize soil amplification for all layering and bedrock acceleration types. By the application of geophysical methods on site, direct measurement of T_{tz} parameter is possible practically. In Fig. 14, AF/T_{tz} ratios were presented for gradually increasing impulsive bedrock accelerations for equal layer thickness model. At bedrock acceleration level 0.005g, linear and concave profiles give a very good correlation for depths $z \geq 20$ m, while convex profiles present a linear relation (i.e. a poor correlation according to *MAE* method, scattering from a horizontal straight line. As the bedrock acceleration level increased to 0.1g, 0.2g, and 0.4g, the correlations for all profiles became closer to a linear straight line (i.e. not a constant line). Also, there is a very distinct transition point between convex and concave profiles. This is true for all bedrock input levels. As the bedrock acceleration level increases, the transition from convex to concave becomes softer. At 0.6g and 1.0g, constant relations were observed just for convex profiles.

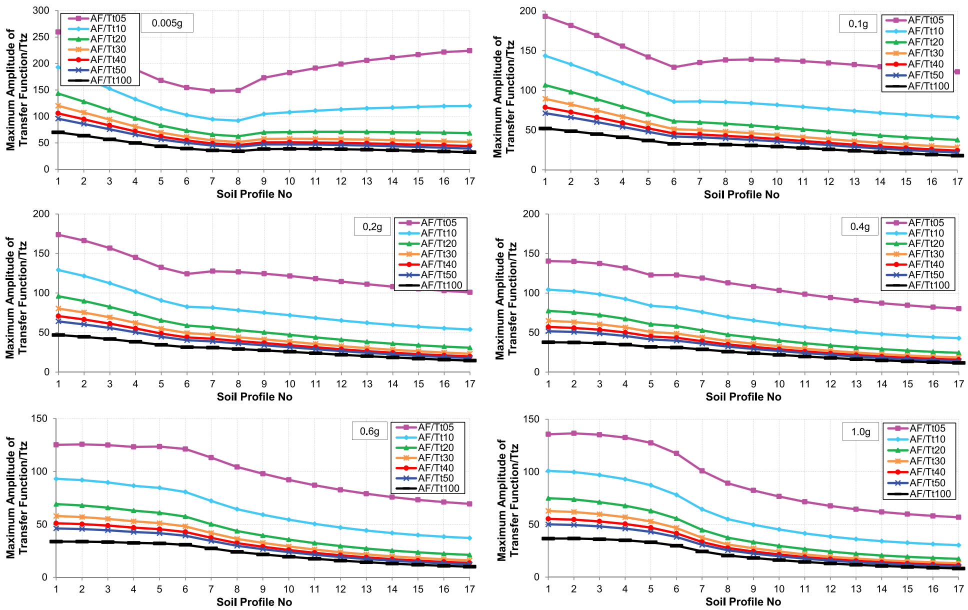

Figure 14. The correlation of AF with T_{tz} for $h = 2$ m, I.

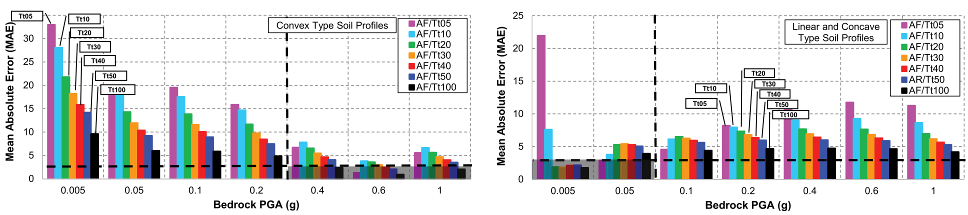

Figure 15. *MAE* values for the correlation of *AF* with T_{tz} for $h = 2$ m, I model; the best performing V_{sz} parameters were labeled in the graph from left to right by an increasing *z*-depth order.

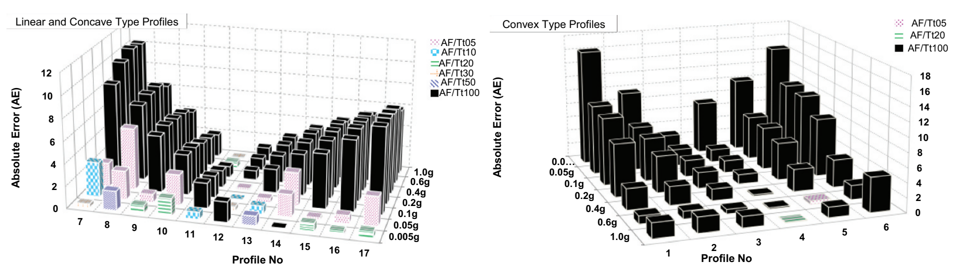

Figure 16. The variation of *AE* for AF/T_{tz} for $h = 2$ m, I.

The correlation of soil amplification parameter T_{tz} is quantified in terms of *MAE* presenting the best performing parameters for each soil profile group by the shaded area in Fig. 15. For each soil profile type, *AE* levels were given in Fig. 16 revealing various *z* parameters based on profile type. Linear and concave profiles presented a good correlation of *AF* and T_{tz} just at $0.005g$ and $0.05g$ bedrock acceleration levels pointing out linear elastic and nonlinear elastic strain ranges. The optimal parameter for convex profiles was T_{t100} for Acc.$\geq$0.4g, and T_{t20} for $0.005g$ and T_{t05} for $0.05g$ for linear/concave profiles.

Table 8. The best performing T_{tz} parameters for soil amplification characterization.

AF/T_{tz}						
Profile Type	Linear/Concave			Convex		
Bedrock PGA	$h = 2$ m, I	$h = 2$ m, W	$t = 0.04$ s, I	$h = 2$ m, I	$h = 2$ m, W	$t = 0.04$ s, I
0.005g	T_{t20}	T_{t10}	T_{t20}	–	–	–
0.05g	T_{t05}	–	T_{t05}	–	–	–
0.1g	–	–	–	–	–	–
0.2g	–	T_{t100}	–	–	T_{t100}	–
0.4g	–	T_{t100}	–	T_{t100}	T_{t100}	T_{tz}
0.6g	–	T_{t100}	–	T_{t100}	T_{t100}	T_{tz} or T_{t50}
1.0g	–	T_{t100}	–	T_{t100}	T_{t100}	T_{tz}

Note: *AF* = soil amplification factor; T_{tz} = shear wave travel time at depth *z*; I = impulsive motion; W= white-noise motion; "*h* = 2 m"= equal layer thickness model; "*t* = 0.04 s"= equal wave travel time model.

According to Table 8, the optimal parameters for all layering models and bedrock acceleration types are identified as follows:

- For linear and concave profiles: T_{t20} or T_{t05} for impulsive Acc. $\leq$0.05g and T_{t100} for white-noise Acc.$\geq$0.2g.
- For convex profiles: T_{t100} for impulsive Acc. $\geq$0.4g and for white-noise Acc. $\geq$0.2g.

It is observed that the correlations by T_{tz} parameters are so changeable for the increasing frequency content of the ground motion that triggers the nonlinearity in soil, for linear and concave profiles. Hence, by considering only the correlations for impulsive bedrock accelerations since they present equal amplitudes of each frequency content (i.e. lower boundary of frequency content), T_{t20} or T_{t05} can be used for the ground accelerations $\leq$0.05g for linear and concave profiles. For convex profiles, T_{t100} and if it is not available, T_{t50}, which is the next best performing parameter for soil amplification characterization, can be used for the ground accelerations $\geq$0.4g in practice.

7.5. Fundamental Frequency Characterization by V_{sz}

The correlation of fundamental soil frequency with time averaged shear wave velocities were investigated at various depths (i.e. V_{s30}, V_{s40}, V_{s50}, and V_{s100}) for gradually increasing bedrock accelerations. The fundamental soil frequencies were observed at the first peaks of transfer functions for linear/concave profiles at all impulsive bedrock accelerations, while they were observed at the third, second, and first peaks as the impulsive bedrock accelerations increased for convex profiles (Table 9). The order of peaks affected the correlations between f_0 and V_{sz} as given in Fig. 17 for equal layer thickness model. At 0.005g bedrock acceleration level, the f_0 was at second peak for Convex-1, at third peak for other convex profiles and at first peak for linear and concave profiles; hence, a sharp transition occurred from profile no. 5 to 6. By gradually increasing the bedrock acceleration level, the higher order peaks (e.g. second and third peaks) are damped and they are shifted towards the first peak. Different order of maximum peaks causes sharp changes in f_0/V_{sz} correlations.

Table 9. The order of maximum peaks at transfer functions for f_0 for $h = 2$ m, I.

Profile No.	Soil Type	0.005g	0.05g	0.1g	0.2g	0.4g	0.6g	1.0g
1	Convex-6	3rd	2nd	2nd	2nd	2nd	2nd	1st
2	Convex-5	3rd	2nd	2nd	2nd	2nd	2nd	1st
3	Convex-4	3rd	2nd	2nd	2nd	2nd	2nd	1st
4	Convex-3	3rd	2nd	2nd	2nd	2nd	1nd	1nd
5	Convex-2	3rd	2nd	2nd	2nd	2nd	1st	1st
6	Convex-1	2nd	2nd	2nd	1st	1st	1st	1st

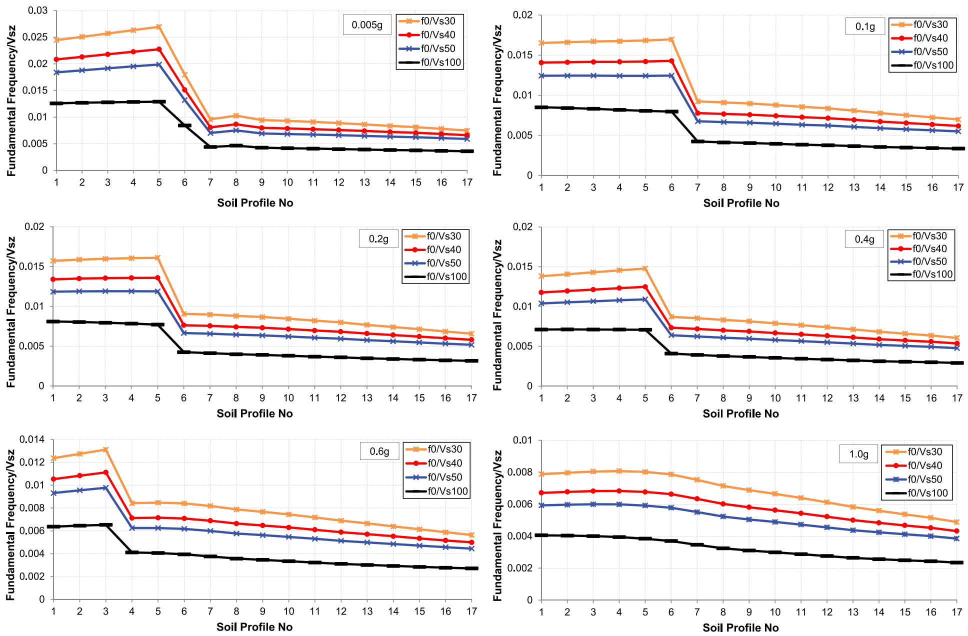

Figure 17. The correlation of f_0 with V_{sz} for impulsive bedrock accelerations for equal layer thickness model.

Table 10. The best performing V_{sz} parameters for f_0 characterization.

	f_0/V_{sz}					
Profile Type	Linear/Concave			Convex		
Bedrock PGA	$h = 2$ m, I	$h = 2$ m, W	$t = 0.04$ s, I	$h = 2$ m, I	$h = 2$ m, W	$t = 0.04$ s, I
0.005g	V_{s100}	V_{s100}	V_{sz} or V_{s50}			
0.05g	V_{s100}	V_{s100}	V_{sz} or V_{s50}	V_{s50}		V_{s50}
0.1g	V_{s100}	V_{s100}	V_{sz} or V_{s50}	V_{s50}		V_{s50}
0.2g	V_{s100}	V_{s100}	V_{sz} or V_{s50}			
0.4g	V_{s100}	V_{s100}	V_{sz} or V_{s50}		V_{s100}	
0.6g	V_{s100}	V_{s100}	V_{sz} or V_{s50}		V_{s100}	
1.0g	V_{s100}	V_{s100}	V_{sz} or V_{s50}	V_{s30} or V_{s40}	V_{s100}	V_{s50} or V_{s40} or V_{s30}

Note: f_0 = fundamental soil frequency; V_{sz}= averaged shear wave velocity at depth z; I= impulsive motion; W= white-noise motion; "$h = 2$ m"= equal layer thickness model; "$t = 0.04$ s"= equal wave travel time model.

Table 10 presents the best performing averaged velocities defined by the lowest *AE* and *MAE* score at various depths for f_0 characterization. The smallest *AE*s were observed at 0.05g, 0.1g, and 1.0g bedrock accelerations for convex profiles, where f_0 was at the same order peaks for all profiles. The correlations for linear and concave profiles were nearly the same; they presented relations closer to a linear line instead of a constant one. The optimal parameters are identified as follows:

- For linear and concave profiles: V_{s100} or V_{s50} as the next best performing parameter for all acceleration types and levels.
- For convex profiles: V_{s50} for impulsive acceleration levels of 0.05g, 0.1g, and 1.0g, and V_{s100} for white-noise Acc. ≥0.4g. It can be generalized that V_{s100} or V_{s50} can be used for bedrock accelerations≥0.05g.

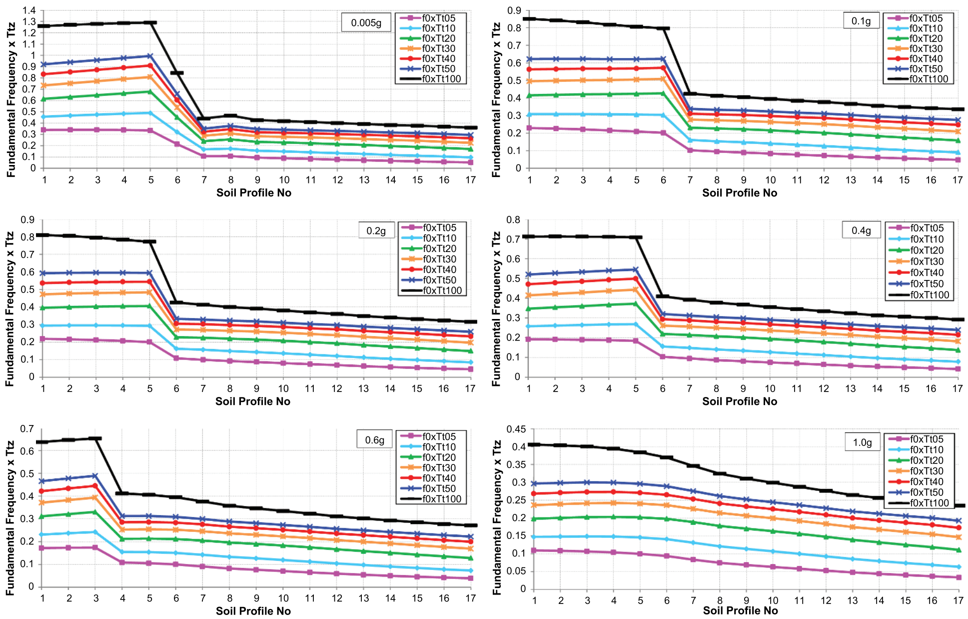

Figure 18. The correlation of f_0 with T_{tz} for $h = 2$ m, I.

7.6. Fundamental Frequency Characterization by T_{tz}

The correlation of f_0 with T_{tz} at various depths were investigated by multiplying f_0 with T_{tz} to check if a constant line can be obtained. The correlations were presented for $h = 2$ m model for impulsive bedrock accelerations in Fig. 18. As in the correlation between f_0 and V_{sz}, the order of f_0 peaks in the transfer functions affected the correlation between f_0 and T_{tz} as well. A distinct transition point was observed for $f_0 x T_{tz}$ correlations between convex and linear/concave profiles because all fundamental frequencies for linear/concave profiles were at the first peak, and for convex profiles at the second/third peaks. As shown in Table 9, the sharp transitions between convex profiles were observed from profile no. 5 to 6 at 0.005*g*, 0.2*g*, and 0.4*g* bedrock acceleration levels and from no. 3 to 4 at 0.6*g* where the order of f_0 is different for the mentioned profiles. As the bedrock acceleration increased, the transition point was softened between convex and linear/concave profile types since the f_0 values of convex profiles were shifted to lower peaks (i.e. from the third to second, and from the second to first peaks). It is observed more constant relations for convex profiles at specific bedrock accelerations where f_0 values were observed at the same order peaks. For linear/concave profiles, the correlations were close to a linear line, rather than

Table 11. The best performing T_{tz} parameters for f_0 characterization.

	$f_0 \times T_{tz}$					
Profile Type	Linear/Concave			Convex		
Bedrock PGA	$h = 2$ m, I	$h = 2$ m, W	$t = 0.04$ s, I	$h = 2$ m, I	$h = 2$ m, W	$t = 0.04$ s, I
0.005*g*	T_{t05}	T_{t05}	T_{t50} or T_{t05}	–	–	–
0.05*g*	T_{t05}	T_{t05}	T_{t05}	T_{t50}	–	T_{t05}
0.1*g*	T_{t05}	T_{t05}	T_{t05}	T_{t50}	–	T_{t05} or T_{t20}
0.2*g*	T_{t05}	T_{t05}	T_{t05}	–	–	–
0.4*g*	T_{t05}	T_{t05}	T_{t05}	–	T_{t20}	–
0.6*g*	T_{t05}	T_{t05}	T_{t05}	–	T_{t05}	–
1.0*g*	T_{t05}	T_{t05}	T_{t05}	T_{t20}	T_{t05}	T_{t05} or T_{t10}

Note: f_0= fundamental soil frequency; T_{tz}= shear wave travel time at depth *z*; I= impulsive motion; W= white-noise motion; "$h = 2$ m"= equal layer thickness model; "$t = 0.04$ s"= equal wave travel time model.

a constant line for all acceleration levels, even so T_{tz} can be used as a characterizing parameter for f_0.

T_{tz} performed well for convex profiles at nonlinear elastic (0.05*g* and 0.1*g*) and elasto-plastic (1.0*g*) strain levels; the most common parameter was T_{t50} among all profiles. T_{t05} had the best performance for linear/concave profiles at all bedrock acceleration levels.

Table 11 shows the performance of T_{tz} at various depths for the characterization of fundamental soil frequency according to *MAE* and *AE* scores. The best performing parameters are identified as follows:

- For linear and concave profiles: T_{t05} for all acceleration types and levels.
- For convex profiles: T_{t50} or T_{t05} for impulsive acceleration levels of 0.05*g*, 0.1*g* and 1.0*g*; and T_{t05} for white-noise Acc. ≥0.4*g*. It can be generalized that T_{t05} can be used for bedrock accelerations ≥ 0.05*g*.

As a general comment, averaged travel time for the top 5 m, T_{t05}, is a good proxy for the f_0 characterization for all type of soil profiles.

7.7. Correlation of Linear and Nonlinear Site Amplification Factors and Fundamental Frequencies

The nonlinear soil response and its correlations with linear soil response were studied for each layering type and increasing bedrock acceleration levels. The objective was to determine if the nonlinear fundamental soil frequencies and soil amplification factors can be estimated from the linear ones by simple means. Fundamental soil frequencies can easily be identified reliably from ambient noise measurements (i.e. by spectral analysis), but not the amplification factors (Atakan 1995; Field and Jacob 1995; Lachet and Bard 1994; Parolai 2012; Safak 1997). Other types of field measurements including reference site methods (e.g. Standard Spectral Ratio and Cross Spectral Ratio) should be used to identify site amplification (Safak 1997). Since ground noise measurements (by microtremors, traffic noise, wind, etc.) correspond to weak motions, hence low shear stresses, the calculated fundamental soil frequencies represent linear soil behavior.

In this study, the linear soil amplification factors and fundamental frequencies are assumed to correspond to those at 0.005*g* bedrock acceleration level. For increasingly higher bedrock acceleration levels, where the soil gradually becomes nonlinear, the correlation was investigated in terms of the ratio of the linear parameters to the nonlinear ones. For both correlations, the ratios for linear/concave

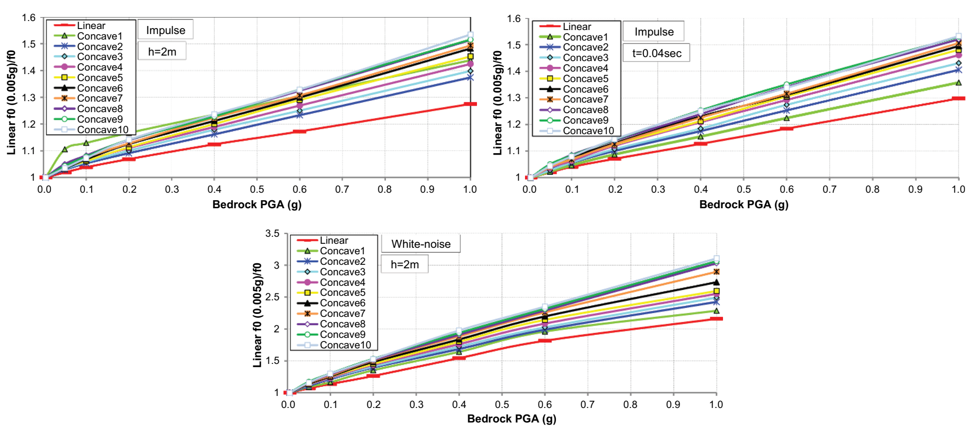

Figure 19. Relation between linear and nonlinear f_0 for linear and concave profiles.

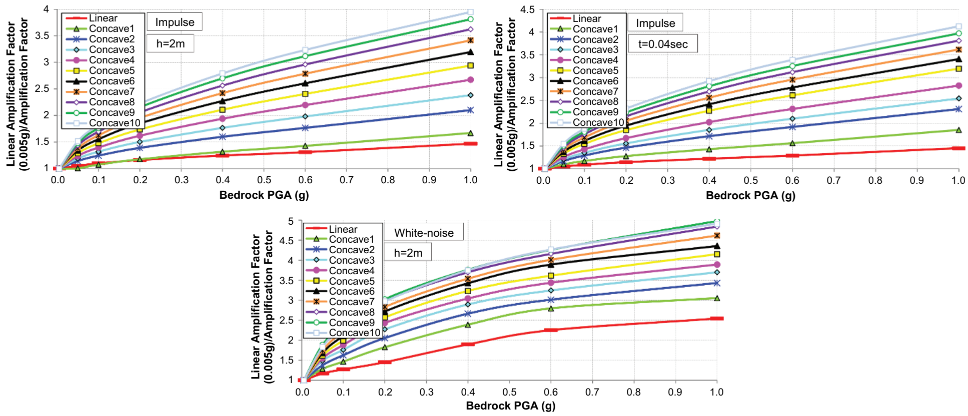

Figure 20. Relation between linear and nonlinear soil amplification for linear and concave profiles.

profiles increased linearly (i.e. increasing nonlinearity) with increasing bedrock PGAs in all three cases, besides an irregular increasing trend was seen for each convex profile (Figs. 19 and 20). Figure 19 shows the linear/nonlinear ratios of fundamental soil frequencies for each profile, layering scheme, bedrock input type, and bedrock acceleration levels. The results of different layering type models by impulse bedrock motion revealed so similar correlations. The degree of nonlinearity for white-noise type accelerations was observed higher than the impulsive type accelerations. The correlations showed that nonlinear fundamental soil frequencies can be estimated from the linear ones only for linear and concave profiles.

The correlation of linear soil amplification factors with the nonlinear ones were presented in Fig. 20. The correlations of amplification factors for both layering models under impulsive and white-noise motion were very similar to those for the fundamental soil frequency. Similarly, the nonlinear soil amplifications can be estimated from the linear ones only for linear and concave profiles. Considering that the linear amplification and fundamental frequency can easily be calculated from field measurements, these guidelines provide a useful tool to estimate the nonlinear ones.

8. Conclusions

A parametric study to investigate the reliability of V_{s30} and some alternative parameters, including time-averaged shear wave velocities, V_{sz}, and wave travel times, T_{tz}, at various depths was carried out to characterize site amplification factor (i.e. *AF*, peak value of spectral ratio amplitudes in this study) and fundamental frequency by constructing convex, linear, and concave profiles. Unlike the previous studies that analyzed seismically instrumented sites including too much variation in data, this study presents a basic and effective approach to investigate the effect of layering type, impedance ratio, and variation of velocity distribution on soil response by constructing theoretical velocity profiles with a single equation. The constructed velocity profiles that are continuously increasing with depth, are defined as D soil class for convex type and E soil class for linear and concave type by V_{s30} according to NEHRP. The most important point distinguishing this study from the previous ones, is the observation of soil response changing from linear to nonlinear and accordingly changing best performed V_{sz} and T_{tz} parameters for soil characterization by gradually increasing bedrock accelerations for various velocity profiles. The significant findings of this study are listed as follows:

(1) The high impedance contrast between the top layers of relatively stiffer convex profiles caused stiff soil amplification by means of increase in surface PGAs which was evaluated as

a theoretical validation of the previous studies (Andreotti and Calvi 2021; Calvi and Andreotti 2022; Mucciarelli and Gallipoli 2006; Xiao et al. 2022) carried out in seismically instrumented sites.

(2) For bedrock accelerations $\leq 0.6g$ (i.e. linear elastic and nonlinear elastic strain ranges), convex profiles have higher f_0, sometimes observed at the second and higher peaks of transfer function, than the ones for linear/concave profiles. They would amplify high frequency portion of ground motions more than the low frequency portions. For linear and concave profiles, f_0 values were observed at the first peaks of transfer functions for all bedrock acceleration levels.

(3) The degradation of soil stiffness occurred more rapidly by white-noise type accelerations compared to impulsive type resulting in lower soil amplification factors, lower fundamental frequencies, higher shear strains, and higher surface PGAs. Thus, the frequency content of bedrock motions is an important factor on nonlinear soil response.

(4) There is a sharp change in the correlations of soil amplification and f_0 with V_{sz}, T_{tz} and surface PGA when switching from convex to concave profiles.

(5) The correlations differ for each bedrock acceleration type (e.g. impulsive and white-noise) and by gradually increasing acceleration levels. However, for different layering schemes under the same bedrock acceleration type (i.e. impulsive), the correlations do not differ.

(6) For convex profiles only, surface PGAs for all bedrock acceleration types $\geq 0.1g$, and fundamental soil frequencies for all bedrock acceleration types $\leq 0.4g$ can be used for the characterization of soil amplification.

(7) Alternative V_{sz} and T_{tz} parameters performed better than V_{s30} to characterize soil amplification.

(8) The soil response varies by the frequency content and gradually increasing amplitude of ground motion due to nonlinearity. It is revealed that whereas some parameters performed well for all strain levels, some others performed well just at limited strains. Hence, this study suggests using different V_{sz} and T_{tz} parameters for varying range of ground motion amplitudes for the characterization of soil amplification and fundamental frequency.

(9) By a conservative approach in practice on site, the optimal parameter to characterize soil amplification is V_{s10} for all bedrock accelerations $\geq 0.2g$ for linear/concave profiles. For convex profiles, the optimal parameter is V_{s100} and then V_{s50} for bedrock accelerations $\leq 0.2g$.

(10) In terms of travel times, the optimal parameters to characterize soil amplification for linear/concave profiles are T_{t20} or T_{t05} for all bedrock accelerations $\leq 0.05g$. For convex profiles, the optimal parameter is T_{t100} and then T_{t50} for all bedrock accelerations $\geq 0.4g$. For convex profiles, V_{s100} performed well for bedrock accelerations $\leq 0.2g$, while T_{t100} performed well for bedrock accelerations $> 0.2g$ to characterize soil amplification. For linear and concave profiles, V_{s10} can be used for bedrock accelerations $\geq 0.2g$, while T_{05} or T_{t20} can be used for bedrock accelerations $\leq 0.05g$.

(11) For linear and concave profiles, fundamental soil frequency can be characterized by V_{s50} or V_{s100} and T_{t05} for all bedrock accelerations (i.e. at linear and nonlinear strains). These parameters can also be used for convex profiles for bedrock accelerations $\geq 0.05g$.

(12) For the profiles considered, nonlinear soil amplification factors and fundamental frequencies can be estimated from the linear ones only for linear and concave profiles. This has a practical significance, since the latter one can be identified from simple field measurements (e.g. ambient noise measurements).

(13) As a result of this study, the optimal parameters presented for linear, concave, and convex profiles show that soil amplification and fundamental frequency characterization should be carried out considering the shear wave velocity distribution with depth and level of earthquake ground motion.

(14) For the utilization of the results of this study in practice, one can approximate any discretely-changing velocity profiles by one of these smoothly changing profiles (i.e. linear, concave, and

convex) constructed in this study and accordingly the best performing V_{sz} and T_{tz} parameter can be chosen due to the shape of the velocity profile.

Disclosure statement

No potential conflict of interest was reported by the author(s).

ORCID

N. Özge Fercan http://orcid.org/0000-0001-6451-1457

Data Availability Statement

All constructed soil profiles, soil models, V_{sz} and T_{tz} parameters used and generated during this study and the correlations of these parameters appear in the submitted article. All the data related to the evaluation method of soil characterization can be reached from the corresponding author upon request.

References

Andreotti, G., and G. M. Calvi. 2021. "Nonlinear Soil Effects on Observed and Simulated Response Spectra." *Earthquake Engineering and Structural Dynamics* 50 (1): 3831–3854. https://doi.org/10.1002/eqe.3535.

Atakan, K. 1995. "A Review of the Type of Data and the Techniques Used in Empirical Estimation of Local Site Response." In *Proceedings of the 5th International Conference on Seismic Zonation*, Vol. II, 1451–1460. Nice, France.

Boore, D. M. 2004. "Estimating Vs30 (Or NEHRP Site Classes) from Shallow Velocity Models (Depths <30 M)." *Bulletin of Seismological Society of America* 94 (2): 591–597.

BSSC (Building Seismic Safety Council). 1997. *NEHRP Recommended Provisions for Seismic Regulations for New Buildings and Other Structures Part 1: Provisions (FEMA 302)*. Washington, D.C: BSSC.

Cadet, H., P. Y. Bard, and A. M. Duval. 2008. "A New Proposal for Site Classification Based on Ambient Vibration Measurements and the KiK-Net Strong Motion Data Set." In *Proceedings of the 14th World Conference on Earthquake Engineering*, Beijing, China. Paper no: 03-01-0036.

Cadet, H., P. Y. Bard, A. M. Duval, and E. Bertrand. 2012. "Erratum To: Site Effect Assessment Using KiK-Net Data: Part 2—Site Amplification Prediction Equation Based on F0 and Vsz." *Bulletin of Earthquake Engineering* 10 (2): 451–489. https://doi.org/10.1007/s10518-011-9324-9.

Calvi, G. M., and G. Andreotti. 2022. "Effects of Local Soil, Magnitude and Distance on Empirical Response Spectra for Design." *Journal of Earthquake Engineering* 26 (3): 1117–1144. https://doi.org/10.1080/13632469.2019.1703847.

Castellaro, S., F. Mulargia, and P. L. Rossi. 2008. "V_{s30}: Proxy for Seismic Amplification?" *Seismological Research Letters* 79 (4): 540–543. https://doi.org/10.1785/gssrl.79.4.540.

CEN (European Committee for Standardization). 2004. *Design of Structures for Earthquake Resistance, Part 1: General Rules, Seismic Actions and Rules for Buildings*. Brussels: Eurocode 8: CEN.

Derras, B., P. Y. Bard, and F. Cotton. 2017. "V_{s30}, Slope, H_{800} and f_0: Performance of Various Site-Condition Proxies in Reducing Ground-Motion Aleatory Variability and Predicting Nonlinear Site Response." *Earth Planets & Space* 69 (133). https://doi.org/10.1186/s40623-017-0718-z.

Field, E. H., and K. H. Jacob. 1995. "A Comparison and Test of Various Site Response Estimation Techniques, Including Three That Are Non-Reference-Site Dependent." *Bulletin of the Seismological Society of America* 85 (4): 1127–1143. https://doi.org/10.1785/BSSA0850041127.

Hashash, Y. M. A., D. R. Groholski, C. A. Philips, and D. Park. 2008. *DEEPSOIL v3.5beta: User Manual and Tutorial* (U. C.: University of Illinois).

Hassani, B., and G. M. Atkinson. 2016. "Applicability of the Site Fundamental Frequency as a V_{s30} Proxy for Central and Eastern North America." *Bulletin of the Seismological Society of America* 106 (2): 653–664. https://doi.org/10.1785/0120150259.

ICBO (International Conference of Building Officials). 1997. *Uniform Building Code*. Vol. 1. California, U.S.A: ICBO.

Kramer, S. L. 1996. *Geotechnical Earthquake Engineering*. New Jersey: Prentice-Hall Upper Saddle River.

Kwak, D. Y., and E. Seyhan. 2020. "Two-Stage Nonlinear Site Amplification Modeling for Japan with V_{S30} and Fundamental Frequency Dependency." *Earthquake Spectra* 36 (3): 1359–1385. https://doi.org/10.1177/8755293020907920.

Lachet, C., and P. Y. Bard. 1994. "Numerical and Theoretical Investigations on the Possibilities and Limitations of Nakamura's Technique." *Journal of Physics of the Earth* 42 (5): 377–397. https://doi.org/10.4294/jpe1952.42.377.

Laurendeau, A., F. Cotton, O. J. Ktenidou, L. F. Bonilla, and F. Hollender. 2013. "Rock and Stiff-Soil Site Amplification: Dependency on V_{s30} and Kappa (κ_0)." *Bulletin of the Seismological Society of America* 103 (6): 3131–3148. https://doi.org/10.1785/0120130020.

Lee, V. W., and M. D. Trifunac. 2010. "Should Average Shear-Wave Velocity in the Top 30 M of Soil Be Used to Describe Seismic Amplification?" *Soil Dynamics and Earthquake Engineering* 30 (11): 1250–1258. https://doi.org/10.1016/j.soildyn.2010.05.007.

Luzi, L., R. Puglia, F. Pacor, M. R. Gallipoli, D. Bindi, and M. Mucciarelli. 2011. "Proposal for a Soil Classification Based on Parameters Alternative or Complementary to V_{s30}." *Bulletin of Earthquake Engineering* 9 (6): 1877–1898. https://doi.org/10.1007/s10518-011-9274-2.

Mucciarelli, M., and M. R. Gallipoli. 2006. "Comparison Between V_{s30} and Other Estimates of Site Amplification in Italy." In *Proceedings of the 1st European Conference on Earthquake Engineering and Seismology*, Geneva, Switzerland. Paper no:270.

Park, D., and Y. M. A. Hashash. 2004. "Probabilistic Seismic Hazard Analysis with Nonlinear Site Effects in the Mississippi Embayment." In *Proceedings of the 13th World Conference on Earthquake Engineering*, Vancouver, Canada. Paper no:1549.

Parolai, S. 2012. "Investigation of Site Response in Urban Areas by Using Earthquake Data and Seismic Noise." In *New Manual of Seismological Observatory Practice 2 (NMSOP-2)*, edited by P. Bormann, 1–38. Potsdam: Deutsches GeoForschungsZentrum, GFZ. https://doi.org/10.2312/GFZ.NMSOP-2.

Regnier, J., L. F. Bonilla, E. Bertrand, and J. F. Semblat. 2014. "Influence of the V_s Profiles Beyond 30 M Depth on Linear Site Effects: Assessment from the KiK-Net Data." *Bulletin of the Seismological Society of America* 104 (5): 2337–2348. https://doi.org/10.1785/0120140018.

Regnier, J., F. Bonilla, A. M. Duval, J. F. Semblat, and E. Bertrand. 2011. "Revisiting V_{s30} as a Proxy Parameter for Site Effects: A Case Study Using KiK-Net Data." In *Proceedings of the 5th International Conference on Earthquake Geotechnical Engineering*. Santiago, Chile.

Regnier, J., H. Cadet, L. F. Bonilla, E. Bertrand, and J. F. Semblat. 2013. "Assessing Nonlinear Behavior of Soils in Seismic Site Response: Statistical Analysis on KiK-net Strong-Motion Data." *Bulletin of the Seismological Society of America* 103 (3): 1750–1770. https://doi.org/10.1785/0120120240.

Safak, E. 1997. "Models and Methods to Characterize Site Amplification from a Pair of Records." *Earthquake Spectra* 13 (1): 97–129. https://doi.org/10.1193/1.1585934.

Seed, H. B., and I. M. Idriss. 1970. *Soil Moduli and Damping Factors for Dynamic Response Analysis*. Report No. UCB/EERC-70/10. Berkeley: University of California.

Steidl, J. H. 2000. "Site Response in Southern California for Probabilistic Seismic Hazard Analysis." *Bulletin of the Seismological Society of America* 90 (6B): 149–169. https://doi.org/10.1785/0120000504.

Stewart, J. P., A. Liu, and Y. Choi. 2003. "Amplification Factors for Spectral Acceleration in Tectonically Active Regions." *Bulletin of the Seismological Society of America* 93 (1): 332–352. https://doi.org/10.1785/0120020049.

TBSC (Turkish Building Seismic Code). 2018. *Ministry of Interior, Disaster and Emergency Management Presidency*. Ankara, Turkey: TBSC.

Tsai, C. C., T. Kishida, and W. C. Lin. 2021. "Adjustment of Site Factors for Basin Effects from Site Response Analysis and Deep Downhole Array Measurements in Taipei." *Engineering Geology* 285:106071. https://doi.org/10.1016/j.enggeo.2021.106071.

Xiao, M., J. Cui, Y. Li, and V. Nguyen. 2022. "Nonlinear Seismic Response Based on Different Site Types: Soft Soil and Rock Strata." *Advances in Civil Engineering* 2022:10. Article ID 5370369. https://doi.org/10.1155/2022/5370369.

Zhao, J. X., and H. Xu. 2013. "A Comparison of VS_{30} and Site Period as Site-Effect Parameters in Response Spectral Ground-Motion Prediction Equations." *Bulletin of the Seismological Society of America* 103 (1): 1–18. https://doi.org/10.1785/0120110251.

Zhu, C., M. Pilz, and F. Cotton. 2020. "Which is a Better Proxy, Site Period or Depth to Bedrock, in Modelling Linear Site Response in Addition to the Average Shear-Wave Velocity?" *Bulletin of Earthquake Engineering* 18 (3): 797–820. https://doi.org/10.1007/s10518-019-00738-6.